

Retraction

Retracted: Design of Remote Real-Time Positioning Method for Long-Distance Running under Wireless Network Technology

Security and Communication Networks

Received 26 December 2023; Accepted 26 December 2023; Published 29 December 2023

Copyright © 2023 Security and Communication Networks. This is an open access article distributed under the Creative Commons Attribution License, which permits unrestricted use, distribution, and reproduction in any medium, provided the original work is properly cited.

This article has been retracted by Hindawi, as publisher, following an investigation undertaken by the publisher [1]. This investigation has uncovered evidence of systematic manipulation of the publication and peer-review process. We cannot, therefore, vouch for the reliability or integrity of this article.

Please note that this notice is intended solely to alert readers that the peer-review process of this article has been compromised.

Wiley and Hindawi regret that the usual quality checks did not identify these issues before publication and have since put additional measures in place to safeguard research integrity.

We wish to credit our Research Integrity and Research Publishing teams and anonymous and named external researchers and research integrity experts for contributing to this investigation.

The corresponding author, as the representative of all authors, has been given the opportunity to register their agreement or disagreement to this retraction. We have kept a record of any response received.

References

- [1] X. Xia, "Design of Remote Real-Time Positioning Method for Long-Distance Running under Wireless Network Technology," *Security and Communication Networks*, vol. 2021, Article ID 5298736, 9 pages, 2021.

Research Article

Design of Remote Real-Time Positioning Method for Long-Distance Running under Wireless Network Technology

Xu Xia 

Hunan University of Humanities Science and Technology, Hunan 417000, China

Correspondence should be addressed to Xu Xia; 164104134@stu.cuz.edu.cn

Received 24 August 2021; Revised 14 September 2021; Accepted 18 September 2021; Published 4 October 2021

Academic Editor: Jian Su

Copyright © 2021 Xu Xia. This is an open access article distributed under the Creative Commons Attribution License, which permits unrestricted use, distribution, and reproduction in any medium, provided the original work is properly cited.

Aiming at the problems of low precision, long time, and poor effect of current remote real-time motion location methods, a long-distance real-time motion location method based on wireless network technology was proposed. Through the analysis of wireless network technology, the basic structure and positioning technology of wireless sensor networks are studied. In addition, this paper adopts the core matrix Isomap node location algorithm based on partial least squares (PLS). The distance of geodesic between long-distance running nodes is used to characterize the dissimilarity between nodes, and the sample contribution rate of the partial least squares method is used to find and eliminate the phenomenon of short circuits in long-distance running fields. High-dimensional feature interval is mapped by centroid transformation and kernel transformation. The experimental results show that the method can improve the positioning accuracy and shorten the positioning time effectively.

1. Introduction

Due to the rapid development of MEMS and wireless communication technology, wireless sensor networks and positioning technology have become the focus of research [1]. With the rapid growth of application requirements such as situational awareness and environmental intelligence and the continuous development of information technology, the demand for obtaining the location information of mobile objects is increasing, and the research of wireless network positioning technology has become one of the hotspots [2]. Using the coverage and bandwidth of the communication network to solve the problems of the reachability and information integrity of people or objects, respectively, location-based services have also emerged. Emergency assistance, intelligent transportation, industrial automation, logistics tracking, data collection, sports venues, and other situations require the first time to obtain the location of objects in the target venue and achieve calibration to achieve motion tracking and information transmission. For the large space occasions in long-distance running, remote real-time positioning of long-distance runners to grasp their dynamic status is an important part of ensuring safety. Therefore, it is

of great significance to study the remote real-time positioning of long-distance running [3].

At present, scholars in related fields have studied motion localization and made great progress. Willmott et al. [4] studied the comparability and reliability of GPS equipment in running related to team sports and calculated the typical measurement error and coefficient of variation between GPS devices for the total distance and peak velocity variables. The total distance and peak speed during straight driving were observed between FieldWiz and the catapult GPS device. The research results show that the data from the FieldWiz GPS device are comparable to established devices. Gomes et al. [5] proposed a human motion and appearance retargeting method in monocular video based on shape perception. The user's body shape is used for retargeting while considering the physical constraints of motion in 3D and 2D image domains. A new video retargeting benchmark dataset was proposed, composed of different videos of human motion with annotations. It is used to evaluate the task of synthesizing human video. The dataset can be used as a public basis for improving tracking progress in this field. The dataset and its evaluation protocol are designed to evaluate retargeting methods under more general and challenging conditions.

This method is effective. However, the above methods still have low positioning accuracy, long time, and poor effect. Ansari [6] proposed an adaptive Kalman filter (KF) algorithm based on the singular spectrum analysis (SSA) prediction method. Reference [7] aims to explore a short-term landslide displacement detection method based on GNSS motion positioning. Short-term landslide monitoring is significant and feasible, and a short-term displacement detection method based on GNSS motion positioning time series segmentation was proposed.

Aiming at the above problems, a remote real-time location method of long-distance running based on wireless network technology is proposed. By analyzing the positioning technology of wireless network technology, combined with PLS, Isomap, and MDS principles, the core matrix isometric mapping node positioning algorithm based on PLS is adopted. The geodesic distance between long-distance running nodes is used to characterize the difference of nodes, eliminate the "short circuit" in long-distance running, map it to the high-dimensional feature interval, and solve the position coordinates of long-distance running nodes to realize long-distance real-time positioning of long-distance running. This method's long-distance real-time positioning effect is good, which can effectively improve the positioning accuracy and shorten the positioning time.

2. Wireless Network Technology

Wireless network technology is the general name of a kind of data transmission network using radio technology. It refers to the network that can realize the interconnection of various communication equipment without wiring. Wireless network technology covers a wide range, including global voice and data networks that allow users to establish long-distance wireless connections and infrared and RF technologies optimized for short-distance wireless connections.

2.1. Classification of Wireless Network Technologies. Wireless networks can be divided into different categories according to various wireless network coverage, different network applications, and different network architectures. The classification of wireless networks will be described in detail from the above three perspectives:

- (1) According to different network coverage, wireless networks can be divided into wireless wide area network (WWAN), wireless local area network (WLAN), wireless metropolitan area network (WMAN), and wireless personal area network (WPAN).
- (2) According to different network applications, wireless networks can be divided into wireless sensor network (WSN), wireless mesh networks, also known as Multi-Hop networks, wearable wireless networks, and wireless body area network (WBAN).
- (3) According to the different topologies of wireless networks, wireless networks can be divided into

different types. As we all know, there are five network topologies in wired networks, namely, Bus, Ring, Star, Tree, and Mesh.

2.2. Features of Wireless Network Technology. The main feature of wireless network is to completely eliminate the limitations of wired network, realize the wireless transmission of information, and make people use the network more freely [8].

- (1) Strong mobility: wireless network transmits network signals by transmitting radio waves. As long as it is within the transmission range, people can use the corresponding receiving equipment to realize the connection to the corresponding network.
- (2) Strong network scalability: the wireless network can connect people through wireless signals at any time. Its network expansion performance is relatively strong, which can effectively realize the expansion of network work and configuration settings, which expands the space range of people's use of the network and improves the use efficiency of the network.
- (3) Simple equipment installation: the wireless network does not need to lay a large number of network cables, but only one wireless network transmitting equipment can be installed. At the same time, it also creates very convenient conditions for later network maintenance and greatly reduces the cost of early installation and later maintenance of the network.

2.3. Wireless Sensor Network Technology. Wireless sensor network (WSN) technology is based on sensor technology. Many static or moving sensors cooperate to sense, collect, and process the obtained object information and finally send this information to the network owner. Many types of sensors constituting the network have gradually moved towards integration, networking, and miniaturization [9].

2.3.1. Wireless Sensor Network Architecture. In wireless sensor networks, the four basic entity objects are the target, sensor node, task management, and sink node. However, as a system, external transmission network, base station, external data processing network, gateway, remote task management unit, and users are essential. The basic structure of wireless sensor network is shown in Figure 1.

In Figure 1, the sensor nodes in the target area are the basic units of wireless sensor networks. These sensor nodes are placed in the monitoring area irregularly. All sensor nodes have the functions of sending and receiving data and analyzing and processing data. Sensor nodes communicate with each other through RF signals, forming a self-organizing network. Among these sensor nodes, different subnets are composed of different types of sensor nodes. If the research is interested in the temperature of the object to be measured, the node is composed of temperature sensors. If the object's humidity

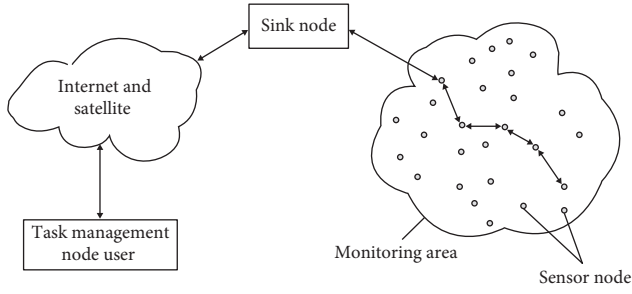


FIGURE 1: Basic structure of wireless sensor network.

needs to be measured, the node is composed of humidity sensors. After the data collection is completed, the information will eventually be transmitted between nodes and aggregated at the sink node.

2.3.2. Node Structure of Wireless Sensor Network. The sensor node in the target area is usually composed of four blocks: sensor unit module, processor and storage unit module, wireless communication unit module, and energy supply unit module. When there are special needs in special occasions, a node mobile positioning module will be added. The node structure of wireless sensor network is shown in Figure 2.

In Figure 2, the processor module is the core of the node, which is responsible for data processing and coordination of various parts and can store data and programs to the memory module. The sensor module is mainly responsible for data collection and processing by the processor. The wireless communication module is responsible for the communication between the node and other nodes. The energy supply module is responsible for providing power support for each part.

2.4. Wireless Sensor Network Positioning Algorithm. The wireless sensor network location algorithm aims to obtain the distance from the reference node to the node to be located. The difference lies in how to obtain the distance. The accuracy of the distance determines the location accuracy. After obtaining the distance, the specific location information is obtained through the solution algorithm. Based on whether direct ranging is needed, it is mainly divided into two kinds: positioning algorithm based on direct ranging and positioning algorithm based on indirect ranging.

2.4.1. Positioning Algorithm Based on Direct Ranging. (1) TOA Positioning Algorithm. When the signal's transmission speed and the signal's transmission time from the transmitting source to the sensing node are known, the distance between the transmitting source and the sensing node can be calculated [10]. Also known as trilateral positioning technology, it has high positioning accuracy. In wireless sensor networks, the coordinates of an unknown node can be determined as long as the distance from an unknown node to three or more beacon nodes is known. The schematic

diagram of the trilateral measurement method is shown in Figure 3.

In a positioning process, suppose there are $n(n \geq 3)$ beacon nodes, the time when the signal is sent from the target is t_0 , the time when it reaches the i beacon node is t_i , the propagation speed of the signal is c , and the coordinates of the target are (x_0, y_0) . If the position of the i beacon node is (x_i, y_i) , then there are

$$\sqrt{(x_0 - x_i)^2 + (y_0 - y_i)^2} = c(t_i - t_0). \quad (1)$$

In formula (1), the target must be on the circle with (x_i, y_i) the center and radius. It is satisfied for any i target node, so the plane position of the target ground can be determined by the intersection of three or more circles.

(2) AOA Positioning Algorithm. The sensor node needs to be equipped with an angle value that can measure the signal of the adjacent beacon node within the communication radius [11]. It is also called the triangulation positioning method or the azimuth positioning method. In-plane conditions, at least two beacon nodes, are required to locate nodes. The schematic diagram of triangulation is shown in Figure 4.

Assume that the coordinates of the beacon node A are (x_1, y_1) , the coordinates of the beacon node B are (x_2, y_2) , the coordinates of the location node C are (x_3, y_3) , and the arrival angles of the signals A and B received by the node C are α and β , respectively. From the geometric properties, it is easy to know that two fixed points and the angled ray determine a point; then, the coordinates of the unknown node C are

$$x = \frac{y_2 - y_1 + x_1 \tan \alpha - x_2 \tan \beta}{\tan \alpha - \tan \beta},$$

$$y = \frac{\tan \alpha y_2 - \tan \beta y_1 + \tan \alpha \tan \beta x_1 - \tan \alpha \tan \beta x_2}{\tan \alpha - \tan \beta}. \quad (2)$$

2.4.2. Location Algorithm Based on Indirect Ranging. The DV-Hop algorithm estimates the distance from the unknown node to the beacon node by the minimum number of hops between the unknown node and the beacon node and uses the product of the average hop distance and the minimum number of hops. Then, the coordinates of unknown nodes are obtained by trilateral measurement principle or maximum likelihood estimation principle [12]. Assume that (x_i, y_i) , (x_j, y_j) are the coordinates of beacon node i, j , and h_{ij} is the number of hops between beacon nodes i, j . The calculation formula for the average hop distance of the beacon node is

$$\text{Hopsize}_i = \frac{\sum_{i \neq j} \sqrt{(x_i - x_j)^2 + (y_i - y_j)^2}}{\sum_{i \neq j} h_{ij}}. \quad (3)$$

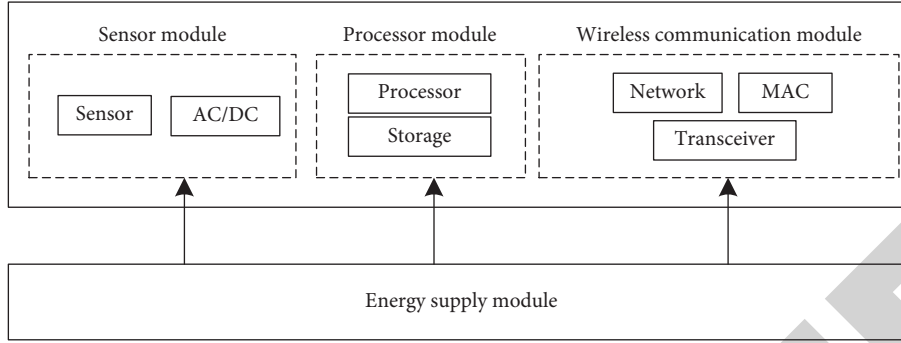


FIGURE 2: The node structure of wireless sensor network.

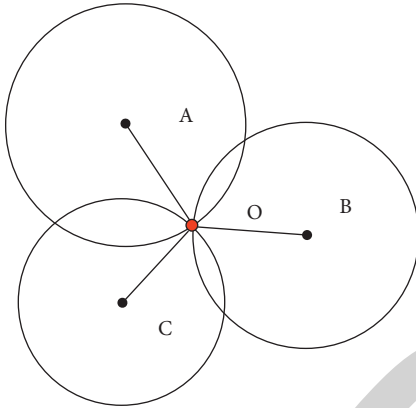


FIGURE 3: Schematic diagram of the trilateral measurement method.

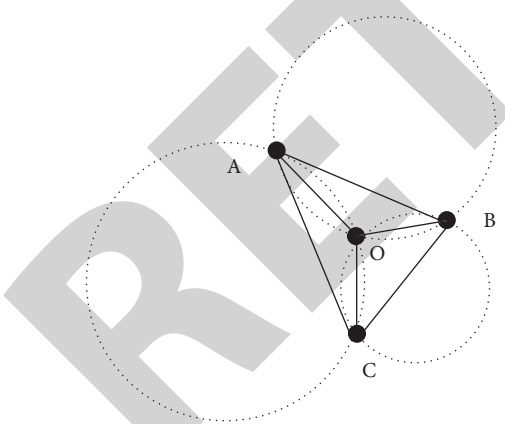


FIGURE 4: Schematic diagram of triangulation method.

After receiving the hop distance, the unknown node calculates the distance of the beacon node according to the recorded hop information by the following formula:

$$d_i = \text{Hopsize}_i \cdot h_i. \quad (4)$$

It can be seen from the above that in DV-Hop algorithm, nodes, the number of beacon nodes, the average connectivity of the network, and the size of the monitoring area are important factors affecting the average hop distance and the

distance from beacon nodes to unknown nodes, thus affecting the positioning accuracy.

3. Long-Distance Running Remote Real-Time Positioning Method

Node localization is one of the key technologies in wireless sensor network applications. In this paper, the core matrix isometric mapping node location algorithm based on PLS is adopted. Combined with the characteristics of PLS, Isomap, and MDS, the long-distance real-time positioning of long-distance running is realized, which has good topological stability, robustness, generalization ability, and positioning accuracy and reduces the computational complexity.

3.1. Relevant Algorithm Principle

3.1.1. Multidimensional Scaling Algorithm. Multidimensional scaling analysis technology optimizes the objective function, obtains the location information of the corresponding points, and reconstructs the topology through the distance relationship between the points or with the phase information such as the relationship. It only needs fewer beacon nodes to achieve more accurate positioning because it makes full use of the existing information between nodes and is suitable for occasions with cooperative positioning [13]. Suppose $X_i = (x_i, y_i, z_i)$ is the coordinate of the sensor node, where $i = 1, 2, \dots, N$. $X = (x, y, z)$ are the coordinates of the target, and the matrices G and h are constructed by the square of the distance between the sensors and the distance between the sensors and the target, as follows:

$$G = \begin{bmatrix} 0 & d_{12}^2 & \cdots & d_{1N}^2 \\ d_{21}^2 & 0 & \cdots & d_{2N}^2 \\ \vdots & \vdots & 0 & \vdots \\ d_{N1}^2 & d_{N2}^2 & \cdots & 0 \end{bmatrix}, \quad (5)$$

$$h = [r_1^2 \ r_2^2 \ \cdots \ r_N^2]^T, \quad (6)$$

where d_{ij} represents the distance between the sensor i, j and r_i represents the distance between the i sensor and the target. Definition:

$$Q = he_N^T + e_N h^T - G, \quad (7)$$

where e_N is the all 1-column vector of $N \times 1$. The construction matrix is as follows:

$$P = \begin{bmatrix} X_1 - X \\ X_2 - X \\ \vdots \\ X_N - X \end{bmatrix} = \begin{bmatrix} x_1 - x & y_1 - y & \cdots & z_1 - z \\ x_2 - x & y_2 - y & \cdots & z_2 - z \\ \vdots & \vdots & \vdots & \vdots \\ x_N - x & y_N - y & \cdots & z_N - z \end{bmatrix}. \quad (8)$$

Available:

$$Q = 2PP^T. \quad (9)$$

From formulas (8) and (9), it can be seen that the rank of matrix Q is 3, and because Q is a symmetric matrix, the singular value decomposition of matrix Q can be performed as follows:

$$Q = U\Lambda U^T, \quad (10)$$

where $\Lambda = \text{diag}(\lambda_1, \lambda_2, \dots, \lambda_N)$ is a diagonal matrix formed by eigenvalues of matrix Q , U is a matrix formed by eigenvectors corresponding to eigenvalues of matrix Q , and U_n is a corresponding noise subspace. The location of the target is

$$\hat{X} = \frac{e_N^T U_n U_n^T}{e_N^T U_n U_n^T e_N} \begin{bmatrix} X_1 \\ X_2 \\ \vdots \\ X_N \end{bmatrix}. \quad (11)$$

3.1.2. Isomap Algorithm. Isometric mapping algorithm is improved based on the multidimensional scaling algorithm. It adopts geodesic distance between nodes instead of Euclidean distance and realizes a nonlinear dimensionality reduction method through double centroid transformation [14]. In the high-dimensional space, suppose $X = \{X_1, \dots, X_m, X_{m+1}, \dots, X_N\}$ is the sensor node set, where $X_i = (x_{i,1}, \dots, x_{i,w})$ is the coordinate of node i , the number of network nodes is N ($N = m + n$), m and n are the number of beacon nodes and unknown nodes in the network, and w is the spatial dimension; then, the Euclidean distance j of nodes i and $d_{i,j}$ is

$$d_{i,j} = \sqrt{\sum_{k=1}^w (x_{i,k} - x_{j,k})^2} = \|x_i - x_j\|_F, \quad (12)$$

where $\|\bullet\|_F$ is the Frobenius norm. Considering the measurement error and noise interference, the actual Euclidean distance $R_{i,j}$ between nodes i and j needs to be corrected as

$$R_{i,j} = d_{i,j} + \xi_{i,j}, \quad (13)$$

where $\xi_{i,j}$ is noise interference and measurement error. The isometric mapping node positioning algorithm constructs a

neighborhood graph. Its similarities and differences use the geodesic distance table between the sample vectors to express the observation data set obtained in the high-dimensional space in the low-dimensional space through the isometric mapping and then use the data for calculation. The linear geometric structure enables the algorithm to achieve nonlinear expansion and high positioning accuracy.

3.1.3. Partial Least Squares. The partial least squares method is a new multivariate statistical data analysis method based on mathematical optimization. The partial least squares method organically combines regression modeling, data structure simplification, and correlation analysis between two groups of variables [15]. The partial least squares method is more similar to factor analysis, splits the X and Y at both ends of the mapping, and uses correlation to sort, which is an extension of the multiple linear regression model. The following formula is its simplest form:

$$Y = b_0 + b_1 X_1 + b_2 X_2 + \cdots + b_n X_n. \quad (14)$$

This equation uses a linear model to describe the relationship between the independent variable Y and the predictor variable group X . In formula (15), the intercept of b_0 is data point 1 to n . The partial least squares regression method is a multiple linear regression method; its purpose is to establish a linear model, and the model is

$$Y = XB + E, \quad (15)$$

where $Y = (y_1, y_2, \dots, y_m)_{n \times m}$, in which m is the number of variables and n is the number of sample points in the response matrix $X = (x_1, x_2, \dots, x_p)_{n \times p}$, in which p is the number of variables and n is the number of sample points of the prediction matrix, E is the noise correction model, and B is the regression coefficient matrix.

3.2. KIsomap Node Location Algorithm Based on PLS Method. PLS-based KIsomap (PLS-KIsomap) node location algorithm is based on Isomap algorithm, uses the contribution rate in PLS-aided analysis method to find and eliminate “short-circuit” edges (outliers) in the neighborhood, improves the algorithm operation efficiency and location accuracy, and then constructs Mercer core matrix according to the idea of core technology to improve the generalization ability of the algorithm. In the high-dimensional feature interval, PLS is used to solve the relative position of long-distance running nodes to further improve its robustness and network topology.

3.2.1. Determination of “Short-Circuit” Side. Its neighborhood size directly determines the topology stability, robustness, and operation efficiency of Isomap algorithm. The generation of “short-circuit” edge is that the neighborhood is too large and destroys the dataset manifold structure, which will make the dataset structure unable to be correctly expressed by the domain, and too small neighborhood will affect the continuity of manifold structure. It is assumed that all sample points have the same contribution to the latent

variables of the dataset, that is, the distribution of sample points in the manifold structure is the same. Let the contribution rate $\text{Cont}_{ij,h}$ of the explanatory variable j of the sample point i in the geodesic distance matrix to the latent variable t_h be

$$\text{Cont}_{ij,h} = \frac{1}{s_h} D_{hj} X_{ij}, \quad (16)$$

where s_h is the standard deviation of the latent variable t_h , $D = (P^T W)^{-1} W^T$, in which P and W are the independent variable load coefficient matrix and the weight coefficient matrix, respectively, and X_{ij} is the observation of the j explanatory variable by the centered i sample point value. Then, the total contribution rate Cont_{ij} of the sample point i to the latent variable t_h ($h = 1, 2, \dots, p$) is

$$\text{Cont}_{ij}^2 = \sum_{h=1}^p \text{Cont}_{ij,h}^2 = \sum_{h=1}^p \left(\frac{1}{s_h} D_{hj} X_{ij} \right)^2. \quad (17)$$

When Cont_{ij}^2 is much larger than the total contribution rate of other sample points or $\text{Cont}_{ij,h}^2$ is much larger than Cont_{ij}^2/p , the sample point i is considered to be a ‘‘short-circuit’’ edge. According to the partial F statistic, the degree of deviation of the sample point from the group is measured, and the problem of selecting a preset value is avoided. By definition:

$$\Delta CC_i = CC_{\sigma(e)} - CC_{\sigma(e,-i)}, \quad (18)$$

where $CC_{\sigma(e)}$ is the variance matrix of the total contribution rate of all the samples, $CC_{\sigma(e,-i)}$ is the variance matrix of the total contribution rate of the samples after deleting the sample point i , and ΔCC_i is the difference between the two. Using ΔCC_i as a statistic to measure the degree of deviation of the contribution rate of sample point i from other sample points [16], construct a partial F statistic:

$$F_i = \frac{\Delta CC_i}{\sigma^2} = \frac{CC_{\sigma(e)} - CC_{\sigma(e,-i)}}{(CC_{\sigma(e)}/(n-p-1))}. \quad (19)$$

That is, the statistic F_i obeys the $F(1, n-p-1)$ distribution. If $F_i \geq F(1, n-p-1)$, the sample point i is considered to be a ‘‘short-circuit’’ edge.

3.2.2. Construction of the Kernel Matrix. Isometric mapping algorithm transforms the linear nonseparable problem in a given space into a linear separable problem in the corresponding high-dimensional feature space through nonlinear mapping. However, it has some shortcomings, such as the selection of nonlinear mapping form and the dimension of feature space; especially when the dimension is high, it will produce ‘‘dimension disaster.’’ The kernel technology is to use the kernel function to replace the inner product operation in the nonlinear mapping, avoiding the problem of mapping form selection and ‘‘dimension disaster.’’ The isometric mapping algorithm is regarded as the kernel principal component analysis (PCA) method [17], and the method of increasing the constant is used to transform K into the Mercer kernel matrix, which can simultaneously ensure the invariance of the geodesic distance and the

semidefiniteness of K . The diagonalization of the kernel matrix is used to obtain low-dimensional embedding of high-dimensional data, which improves the generalization ability of the algorithm.

Let c^* be the maximum eigenvalue of matrix $\begin{bmatrix} 0 & 2K(D^2) \\ -I & -4K(D) \end{bmatrix}$, and take $c \geq c^* \geq 0$; then the geodesic distance matrix D_G after transformation is

$$\tilde{D}_{ij} = D_{ij} + c(1 - \delta_{ij}), \quad (20)$$

where δ_{ij} is the Kronecker delta function. After double centroid transformation, the corresponding Mercer kernel matrix \tilde{K} of K is

$$\tilde{K} = K(\tilde{D}^2) + 2cK(\tilde{D}) + \frac{1}{2}c^2H. \quad (21)$$

According to the Mercer kernel matrix definition, \tilde{K}_{ij} can be expressed as

$$\tilde{K}_{ij} = k(x_i, x_j) = \Phi^T(x_i)\Phi(x_j), \quad (22)$$

where $\Phi(\cdot)$ is a nonlinear mapping form.

3.2.3. Solution of Relative Position of Long-Distance Running Nodes. The isometric mapping node location algorithm can be expressed as the following optimization problem:

$$\min_{D^* \in EDM} \|K - K^*\|_F^2, \quad (23)$$

where EDM is the geodesic distance matrix set and K^* is the corresponding low-dimensional space reconstruction matrix of K . The essence of formula (23) is to use the LS method to solve the semidefinite programming (SDP) problem, usually using the matrix singular value decomposition method. The following is the covariance matrix of N sample points in the high-dimensional feature space:

$$C = \frac{1}{N} \Phi(H)\Phi^T(H). \quad (24)$$

First, the matrix C is decomposed by eigenvalue, and then the corresponding eigenvector matrix is normalized to obtain the relative position coordinates of the sample points in the eigenspace. Assuming that the measurement error and noise interference in D_G obey the Gaussian distribution, after double centroid transformation, the element \tilde{K}_{ij} in the kernel matrix \tilde{K} is

$$\tilde{K}_{ij} = -\frac{1}{2} \left(\tilde{D}_{ij}^2 - \tilde{K}_{jj} - \frac{1}{n} \sum_{i=1}^n \tilde{D}_{ij}^2 - \tilde{K}_{ii} \right). \quad (25)$$

It can be seen from formula (25) that the elements of matrix \tilde{K} no longer obey the Gaussian distribution but present a mixed distribution. At the same time, the noise error between the long-distance running nodes spreads to other nodes and causes noise pollution. When the partial least squares method is used to solve formula (26), it can be expressed as the following optimization problem:

$$\begin{aligned} \max: & \quad T_r\{U^T CV\}, \\ \text{subject to:} & \quad U^T U = V^T V = I, \end{aligned} \quad (26)$$

where U and V are the eigenvector matrices of the high-dimensional feature (dual) space, respectively. In the PLS-KIsomap algorithm, the input matrix X in the regression model is the kernel matrix \tilde{K} , and the PLS method evolved into the kernel partial least squares (KPLS) method, which is transformed into the following optimization problem:

$$\begin{aligned} \max: & \quad T_r\{U^T \Phi^T K^* V\}, \\ \text{subject to:} & \quad U^T U = V^T V = I. \end{aligned} \quad (27)$$

The partial least squares method adopts the nonparametric estimation method, which avoids the problem of strict parameter requirements, has no distribution requirements for the sample data, and can get the asymptotic correct estimation. PLS-KIsomap algorithm combines the advantages of partial least squares and kernel technology to realize the extension of partial least squares linear regression to high-dimensional nonlinear space. At the same time, in the regression model, the centroid matrix is used as the input matrix to eliminate the influence of bias term, reduce the dimension of regression coefficient matrix, and reduce the computational complexity. Through the above steps, the remote real-time positioning of long-distance running is realized.

4. Experimental Simulation and Analysis

4.1. Setting Up the Experimental Environment. In order to verify the effectiveness of the long-distance running remote real-time positioning method under the wireless network technology, the wireless WiFi module used in this article is HF-LPB100-0 low-power embedded wireless module, and its peripheral circuit is designed and mass-produced which greatly reduces hardware deployment cost. The WiFi module designed in this paper enables other devices to connect to the wireless network, integrates MAC, baseband chips, power amplifiers, etc., and finally realizes the deployment of a smart environment for remote real-time positioning of long-distance running. The wireless parameters of the HF-LPB100 module are given in Table 1.

Select 236 people as the long-distance running remote real-time positioning research object. The Windows system is used as the operating platform, and the vector graphics technology is used to provide users with a visual operating interface. The sensor network nodes are assumed to be deployed in a $400 \text{ m} \times 400 \text{ m} \times 2 \text{ m}$ space and the network is fully connected.

4.2. Comparison of Remote Real-Time Positioning Effects of Long-Distance Running. In order to verify the long-distance running remote real-time positioning effect of the proposed method, the proposed method, the methods in reference [4], and the methods in reference [5] were used to compare, and the comparison results of the long-distance real-time positioning effect of different methods are shown in Figure 5.

TABLE 1: Wireless parameters of HF-LPB100 module.

Parameter	Value
Standard certification	FCC/CE
Wireless standard	802.11 b/g/n
Transmit power	11–18 dBm
Receiving sensitivity	–93 dBm ~ –82 dBm
Antenna	External I-PEX connector

It can be seen from Figure 5 that in the node surface layout scene, the node surface position of the methods in reference [4] and the methods in reference [5] deviates greatly from the actual position of the node, while the node surface position of the proposed method is close to the actual position of the node. It can be seen that the long-distance real-time positioning effect of the methods in reference [4] and the methods in reference [5] is poor, while the long-distance real-time positioning effect of the proposed method is relatively good.

4.3. Comparison of Remote Real-Time Positioning Accuracy of Long-Distance Running. On this basis, in order to further verify the positioning accuracy of the proposed method, the average positioning error is used as the evaluation index. The smaller the positioning error, the greater the positioning accuracy of the method. The calculation formula is as follows:

$$E_r = \frac{\sum_{i=m+1}^N \|x_{e,i} - x_{r,i}\|^2}{(N - m) \times r} \times 100\%, \quad (28)$$

where N is the number of sensor network nodes, r is the node communication radius, $x_{e,i}$ and $x_{r,i}$ are the estimated and actual positions of node i , and m is the number of beacon nodes. The proposed method, the methods in reference [4], and the methods in reference [5] are used to carry out long-distance running remote real-time positioning, respectively, and the comparison results of long-distance running real-time positioning errors of different methods are shown in Figure 6.

It can be seen from Figure 6 that with the increase of sampling times, the remote real-time positioning error of long-distance running sports of different methods increases. When the sampling times are 25, the long-distance real-time positioning error of the method in reference [4] is 10.8 m and the long-distance real-time positioning error of the method in reference [5] is 8.6 m, while the long-distance real-time positioning error of the proposed method is only 4.5 m. Therefore, the remote real-time positioning error of the proposed method is small, and the proposed method can effectively improve the remote real-time positioning accuracy of long-distance running.

4.4. Comparison of Remote Real-Time Positioning Time for Long-Distance Running. To further verify the positioning time of the proposed method, the proposed method, the

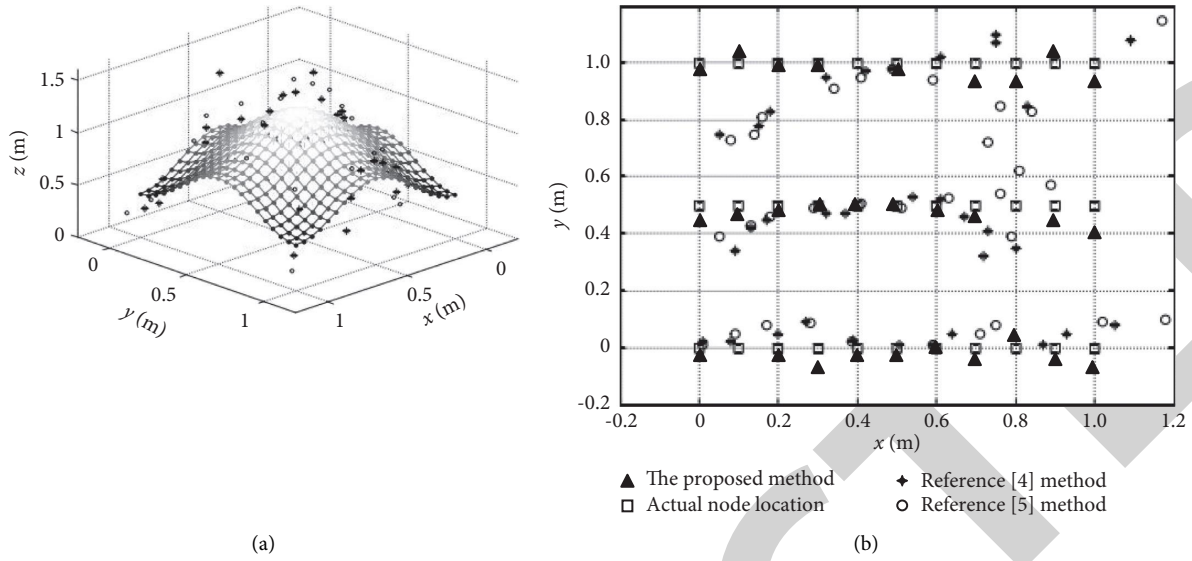


FIGURE 5: Comparison results of remote real-time positioning effects of different methods of long-distance running. (a) 3D drawing of positioning effect in node surface layout scene. (b) X-Y plane projection of positioning effect.

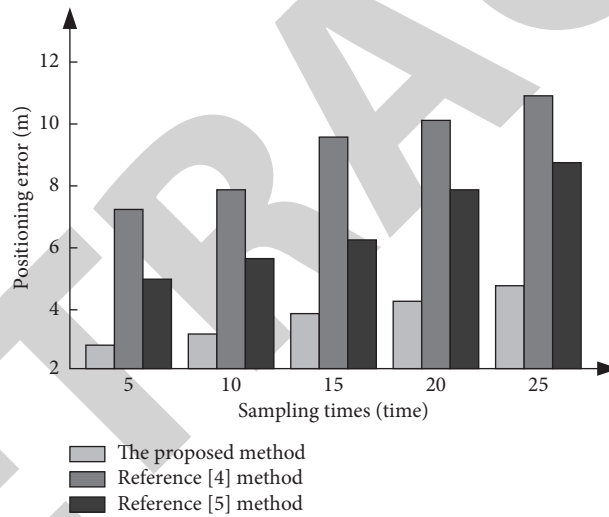


FIGURE 6: Comparison results of remote real-time positioning errors of different methods for long-distance running.

TABLE 2: Comparison results of remote real-time positioning time of different methods of long-distance running.

Sampling times/time	The proposed method/s	The method in reference [4]/s	The method in reference [5]/s
5	10.5	14.8	18.9
10	15.8	19.7	25.3
15	18.6	26.3	29.9
20	23.5	32.2	38.1
25	26.9	38.4	43.7

method of reference [4], and the method of reference [5] are compared and analyzed, and the comparison results of the long-distance running remote real-time positioning time of different methods are given in Table 2.

It can be seen from the data in Table 2 that with the increase of sampling times, the long-distance real-time positioning time of different methods increases. When the

sampling times are 25, the long-distance real-time positioning time of the method in reference [4] is 38.4 s, the long-distance real-time positioning time of the method in reference [5] is 43.7 s, and the long-distance real-time positioning time of the proposed method is 26.9 s. Therefore, the long-distance real-time positioning time of the proposed method is short.

5. Conclusion

The long-distance real-time positioning method proposed in this paper can effectively improve the long-distance real-time positioning accuracy, shorten the long-distance real-time positioning time, and ensure the long-distance real-time positioning effect. However, in this paper, the node energy, hardware resources, and functions in wireless sensor networks are limited, which makes the long-distance real-time location algorithm of long-distance running limited. Long-distance running is different and more complex in various occasions. There is no commonly used algorithm, which can only be used for specific environment. Therefore, in the following research, we need to deeply study the effective algorithms for more long-distance real-time positioning environment, which can realize environment perception and sensitive branch point identification and judgment.

Data Availability

The data used to support the findings of this study are available from the corresponding author upon request.

Conflicts of Interest

The author declares that there are no conflicts of interest.

References

- [1] W. Wang and M. Zhang, "Self-adaptive gathering for energy-efficient data stream in heterogeneous wireless sensor networks based on deep learning," *IEEE Wireless Communications*, vol. 27, no. 5, pp. 74–79, 2020.
- [2] A. Brighente, F. Formaggio, G. M. Di Nunzio, and S. Tomasin, "Machine learning for in-region location verification in wireless networks," *IEEE Journal on Selected Areas in Communications*, vol. 37, no. 11, pp. 2490–2502, 2019.
- [3] A. S. Devyatisil'Nyi and A. V. Shurygin, "Modeling the system of determination of the motion of a technological platform using GLONASS positioning and newtonometry data," *Technical Physics Letters*, vol. 45, no. 9, pp. 920–923, 2019.
- [4] A. G. B. Willmott, C. A. James, A. Bliss, R. A. Leftwich, and N. S. Maxwell, "A comparison of two global positioning system devices for team-sport running protocols," *Journal of Biomechanics*, vol. 83, pp. 324–328, 2019.
- [5] T. L. Gomes, R. Martins, J. Ferreira, R. Azevedo, and E. R. Nascimento, "A shape-aware retargeting approach to transfer human motion and appearance in monocular videos," *International Journal of Computer Vision*, vol. 129, no. 2, pp. 2057–2075, 2021.
- [6] K. Ansari, "Real-time positioning based on Kalman filter and implication of singular spectrum analysis," *IEEE Geoscience and Remote Sensing Letters*, vol. 18, no. 1, pp. 58–61, 2020.
- [7] N. Shen, L. Chen, L. Wang et al., "Short-term landslide displacement detection based on GNSS real-time kinematic positioning," *IEEE Transactions on Instrumentation and Measurement*, vol. 70, pp. 1–14, 2021.
- [8] R. Cavallari, S. Toumpis, R. Verdona, and I. Kontoyiannis, "Packet speed and cost in mobile wireless delay-tolerant networks," *IEEE Transactions on Information Theory*, vol. 66, no. 9, pp. 5683–5702, 2020.
- [9] P. Wu, F. Xiao, C. Sha, H. Huang, and L. Sun, "Trajectory optimization for UAVs' efficient charging in wireless rechargeable sensor networks," *IEEE Transactions on Vehicular Technology*, vol. 69, no. 4, pp. 4207–4220, 2020.
- [10] W. Zhang, G. Han, X. Wang, M. Guizani, K. Fan, and L. Shu, "A node location algorithm based on node movement prediction in underwater acoustic sensor networks," *IEEE Transactions on Vehicular Technology*, vol. 69, no. 3, pp. 3166–3178, 2020.
- [11] F. Jiang and Z. Zhang, "An improved underwater TDOA/AOA joint localisation algorithm," *IET Communications*, vol. 15, no. 6, pp. 802–814, 2021.
- [12] A. Neri, M. Carli, and F. Battisti, "A maximum likelihood approach for depth field estimation based on epipolar plane images," *IEEE Transactions on Image Processing*, vol. 28, no. 2, pp. 827–840, 2019.
- [13] M. Chung and W.-K. Loh, " α -Probabilistic flexible aggregate nearest neighbor search in road networks using landmark multidimensional scaling," *The Journal of Supercomputing*, vol. 77, no. 2, pp. 2138–2153, 2021.
- [14] R. M. Barnett, M. Murphy, and C. V. Deutsch, "A grid mapping algorithm for modeling with geometric transforms," *Computers & Geosciences*, vol. 126, pp. 9–20, 2019.
- [15] G. Xiao, X. Wan, L. Wang, and S. Liu, "Reflectance spectra reconstruction from trichromatic camera based on kernel partial least square method," *Optics Express*, vol. 27, no. 24, pp. 34921–34936, 2019.
- [16] H. Liang, H. Lu, K. Feng, Y. Liu, J. Li, and L. Meng, "Application of the improved NOFRFs weighted contribution rate based on KL divergence to rotor rub-impact," *Nonlinear Dynamics*, vol. 104, no. 4, pp. 3937–3954, 2021.
- [17] F. Yang, "Simulation of adaptive dimension reduction algorithms for hyperspectral images under PCA transform," *Computer Simulation*, vol. 36, no. 8, pp. 441–444 + 450, 2019.